

Demonstration of Joint Communication and Sensing with Fully Digital Arrays

Jan Adler, Jens Kugelmann, Maximilian Matthe, Padmanava Sen

Barkhausen Institut

Dresden, Germany

{jan.adler, jens.kugelmann, maximilian.matthe, padmanava.sen}@barkhauseninstitut.org

Abstract—This hardware demonstration showcases a fully digital mono-static joint communication and sensing approach for multi-antenna arrays. Using a software defined radio testbed consisting of two units transmitting and receiving standard communication waveforms in an in-band full duplex fashion over multiple antennas, it is shown that a range-angle radar image can be estimated from environmental scattering without impacting the communication performance. Such an approach can be key enabler for joint communication and sensing deployment using communication network infrastructure.

I. INTRODUCTION

With the the push towards Joint Communication and Sensing (JCAS), converging sensing and communication functionalities into unifying systems, communication base stations may be enabled to offer mono-static sensing as a service, estimating spatial information about their surroundings in addition to fulfilling their core role of offering communication services to mobile devices [1]. Sensing and communications traditionally rely on different signal processing techniques and exhibit noticeable differences in radio-frequency (RF) front-end designs [2]. Apart from hardware challenges to overcome, such as suppressing transmit-receive leakage in highly integrated antenna arrays [2], the search for waveforms [3] and accompanying signal processing techniques [4] for simultaneously carrying communication information and for enabling the estimation of environment parameters has received significant attention by the research community. Such parameters may include the detection of objects in the base stations' vicinity and the estimation of respective ranges, velocities and positional angles. However, it is unclear if existing industry standards will adopt new waveforms or RF designs simply for the sake of enabling sensing as an additional service. An alternative is the development of communication-centric JCAS, relying on already existing standard-compliant communication waveforms and RF front-ends for both sensing and communication applications. With the adoption of Multiple Input Multiple Output (MIMO) in order to overcome losses in higher frequency bands, minimize interference and increase data capacity, future communication-centric JCAS systems will have access to multiple transmitting and receive-

ing antennas. This demonstration showcases a proof of concept for communication-centric JCAS in fully digital multi-antenna base-stations transmitting well-established communication waveforms and estimating a range-angle radar image from environmental scattering in a simultaneous transmit and receive, in-band full duplex (IBFD) fashion.

II. SIGNAL PROCESSING

The considered system consists of a fully digital antenna array of arbitrary topology featuring N transmitting and M receiving antennas operating at carrier frequency f_c , where each transmitting antenna is being fed by a dedicated RF chain and each receiving antenna feeds into a dedicated RF chain, respectively. A single arbitrary communication frame

$$s(t) \in \mathbb{C} \quad \text{with} \quad s(t) = 0 \quad \text{for} \quad t \notin [0, T_F] \quad (1)$$

of duration T_F is digitally precoded by the transmit beamforming weights $\mathbf{w} \in \mathbb{C}^N$, resulting in $\mathbf{x}(t) = \mathbf{w}s(t)$ representing the base-band signals feeding into the transmitting RF chains. The antenna array's far-field of view is assumed to be populated by L point-like targets scattering the emitted waveform back to the array. Neither the antenna array nor the targets are assumed to be moving. With respect to the antenna array, each target is located at coordinates

$$r_\ell \in [0, R_{\text{Max}}], \quad \phi_\ell \in [0, 2\pi), \quad \theta_\ell \in \left[0, \frac{\pi}{2}\right] \quad (2)$$

in a spherical system spanning the positive half-space in cartesian z-direction, r_ℓ denoting the distance between the array and the target, ϕ_ℓ denoting the azimuth angle and θ_ℓ denoting the zenith angle. A planar wave originating at a far-field target location and impinging onto the antenna array results in the phase response

$$\mathbf{a}_{\text{Tx}}(\phi, \theta) = \left[e^{-j\mathbf{k}^\top(\phi, \theta)\mathbf{p}_1}, \dots, e^{-j\mathbf{k}^\top(\phi, \theta)\mathbf{p}_N} \right]^\top \in \mathbb{C}^N \quad (3)$$

$$\mathbf{a}_{\text{Rx}}(\phi, \theta) = \left[e^{-j\mathbf{k}^\top(\phi, \theta)\mathbf{q}_1}, \dots, e^{-j\mathbf{k}^\top(\phi, \theta)\mathbf{q}_M} \right]^\top \in \mathbb{C}^M \quad (4)$$

at transmitting and receiving antennas, respectively. The phase depends on the individual transmit and receive antenna element positions $\mathbf{p}_n, \mathbf{q}_m \in \mathbb{R}^3$ within the antenna array and the wave vector

$$\mathbf{k}(\phi, \theta) = \frac{2\pi f_c}{c_0} [\sin \theta \cos \phi, \sin \theta \sin \phi, \cos \theta]^\top. \quad (5)$$

This work was financed with tax revenue on the basis of the budget approved by the Saxon state parliament and the European Union's Horizon Europe SNS project INSTINCT (grant agreement no. 101139161).

Adopting the shorthand notations $\mathbf{a}_{\text{Tx/Rx},\ell} = \mathbf{a}_{\text{Tx/Rx}}(\phi_\ell, \theta_\ell)$, the base-band signal emerging from the receiving RF chains can be described as a superposition

$$\mathbf{y}(t) = \sum_{\ell=1}^L \gamma_\ell \mathbf{a}_{\text{Rx},\ell} \mathbf{a}_{\text{Tx},\ell}^H \mathbf{x}(t) * \delta(t - \frac{2r_\ell}{c_0}) + \mathbf{n}(t) \quad (6)$$

$$= \sum_{\ell=1}^L \tilde{\gamma}_\ell \mathbf{a}_{\text{Rx},\ell} s(t - \frac{2r_\ell}{c_0}) + \mathbf{n}(t) \quad (7)$$

of all scattering targets with additive white Gaussian noise $\mathbf{n} \sim \mathcal{N}(0, \mathbf{I}_M \sigma^2)$, where γ_ℓ denotes the target reflectivity and propagation losses and $\tilde{\gamma}_\ell = \gamma_\ell \mathbf{a}_{\text{Tx},\ell}^H \mathbf{w}$ additionally incorporates the antenna array's transmit beamforming characteristics towards the ℓ -th scatterer. After digital sampling of the received base-band waveform at an interval of T_s , an estimate of $\tilde{\gamma}_\ell$ for any candidate target location (r, ϕ, θ)

$$\hat{\gamma}(r, \phi, \theta) = \frac{1}{MK} \sum_{k=0}^{K-1} s^*(kT_s - \frac{2r}{c_0}) \mathbf{a}_{\text{Rx}}^H(\phi, \theta) \mathbf{y}(kT_s) \quad (8)$$

can be exploited to derive a radar image of the surrounding, with peaks in the absolute values of $\hat{\gamma}(r, \phi, \theta)$ indicating possible target locations, while the communication waveform $s(t)$ can be freely selected.

III. DEMONSTRATION

The setup demonstrating the approach described in the previous section consists of two Ettus x410 [5] Software Defined Radios (SDRs), operating at a carrier frequency of $f_c = 6$ GHz, synchronized by a common hardware clock. One SDR unit, representing a multi-antenna base station, is connected to a horn antenna array featuring three transmitting and two receiving antennas, respectively, while the other SDR unit, representing a mobile terminal, is connected to a single transmitting and a single receiving horn antenna focusing the array, so that both arrays face each other at a distance of approximately three meters. Figure 1 depicts the described setup with the base-station to the left and the mobile terminal to the right. The base station can be configured to transmit



Fig. 1: Demo Setup

a selection of standard communication waveforms $s(t)$, such as several filtered single-carrier modulations, orthogonal frequency division multiplexing, orthogonal code division multiplexing and orthogonal time frequency space modulation, as

well as respective parameters such as the modulation order, signal bandwidth and waveform-specific post-processing algorithms for synchronization, channel estimation and channel equalization. Simultaneously, the base station estimates a radar image of its field of view by equation (8) from power backscattered by its environment and subsequently picked up by the receiving antennas. At the mobile terminal, the received waveform is demodulated and unmapped. By comparison with the information transmitted by the base-station communication performance indicators such as error vector magnitude, bit error rates, frame error rates and theoretical data throughput are estimated. The described configuration options, as well as the radar information, communication performance indicators and visualization of the transmitted and received base-band waveforms are accessible and visualized on a touch screen located in between the base station and mobile terminal and can be freely adjusted by visitors of the demonstrator. Figure 2 displays the respective graphical user interface. The underlying base-band signal processing is

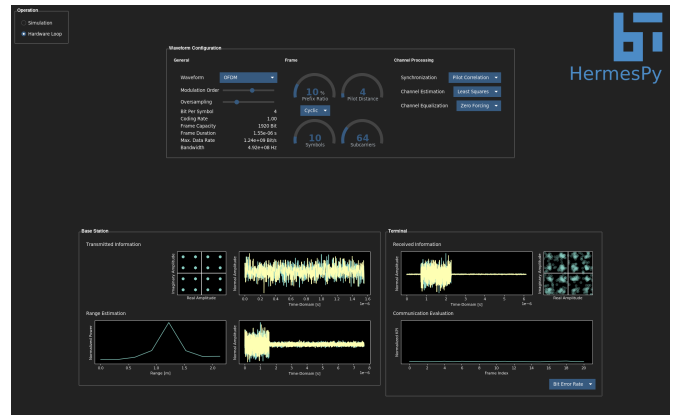


Fig. 2: Control Interface

based on an extension of the the Heterogeneous Radio Mobile Simulator Python (HermesPy) [6] and computed on a central compute unit connected to both SDRs via Ethernet.

REFERENCES

- [1] T. Wild, V. Braun, and H. Viswanathan, "Joint Design of Communication and Sensing for Beyond 5G and 6G Systems," *IEEE Access*, vol. 9, pp. 30 845–30 857, 2021.
- [2] F. Bozorgi, P. Sen, A. N. Barreto, and G. Fettweis, "RF Front-End Challenges for Joint Communication and Radar Sensing," in *2021 1st IEEE International Online Symposium on Joint Communications & Sensing (JC&S)*. IEEE, 2021, pp. 1–6.
- [3] Z. Xiao and Y. Zeng, "Waveform Design and Performance Analysis for Full-Duplex Integrated Sensing and Communication," *IEEE Journal on Selected Areas in Communications*, vol. 40, no. 6, pp. 1823–1837, 2022.
- [4] J. A. Zhang, F. Liu, C. Masouros, R. W. Heath, Z. Feng, Le Zheng, and A. Petropulu, "An Overview of Signal Processing Techniques for Joint Communication and Radar Sensing," *IEEE Journal of Selected Topics in Signal Processing*, vol. 15, no. 6, pp. 1295–1315, 2021.
- [5] NI, "Ettus USRP X410 Specifications," 2024-03-22. [Online]. Available: <https://www.ni.com/docs/en-US/bundle/ettus-usrp-x410-specs/page/specs.html>
- [6] J. Adler, T. Kronauer, and A. N. Barreto, "HermesPy: An Open-Source Link-Level Evaluator for 6G," *IEEE Access*, vol. 10, pp. 120 256–120 273, 2022.